Wiley Encyclopedia of Electrical and Electronics Engineering

Volume 5

John G. Webster, Editor
Department of Electrical and Computer Engineering
University of Wisconsin–Madison

A Wiley-Interscience Publication
John Wiley & Sons, Inc.
New York · Chichester · Weinheim · Brisbane · Singapore · Toronto

Editorial Staff

Editor: John G. Webster

Publisher: Kim H. Kelly

Sponsoring Editor: George J. Telecki

Managing Editor: Kimi J. Sugeno

Logo designed by Gottlieb John Marmet.

This book is printed on acid-free paper. ♾

Published simultaneously in Canada.

For ordering and customer service, call 1-800-CALL-WILEY.

Library of Congress Cataloging-in-Publication Data:
Wiley Encyclopedia of electrical and electronics engineering / John G. Webster, editor.
p. cm.
Includes index.
ISBN 0-471-13946-7 (set : cloth : alk.paper)
1. Electric engineering–Encyclopedias. 2. Electronics–Encyclopedias. I. Webster, John G., 1932-
TK9 .E53 1999
621.3'03–dc21

98-44761
CIP

Printed in the United States of America

10 9 8 7 6 5 4 3 2 1

CONCLUDING REMARKS AND PROSPECTIVE DEVELOPMENTS

In this article we have inspected the mismatches and drift effects on the performance of dc amplifiers implemented from op-amps. Bipolar and MOS differential inputs stages have successively been analyzed. NPN and NMOS transistors have only been considered above. Nevertheless differential amplifiers can also be implemented from PNP or PMOS elements. In these cases note that PNP transistors exhibit lower β values and the mobility of PMOS transistors is about three times smaller.

The general criterion to consider for implementing dc amplifiers and the most commonly used techniques to reduce dc errors have been investigated.

As indicated, dc amplifiers can also be designed from other available building blocks: Traditionally all these dc amplifier implementations use voltage input signals. Rushing into the opening created by the introduction of the CFOA, another design approach could consist in using current input signals in place of voltages.

Second-generation current conveyors can be driven from current signals and these could certainly be used advantageously in designing dc amplifiers.

BIBLIOGRAPHY

1. A. S. Sedra and K. Smith, *Microelectronics Circuits,* 4th ed., New York: Oxford Univ. Press, 1998.
2. Horowitz and W. Hill, *The Art of Electronics,* 2nd ed., New York: Cambridge University Press, 1989.
3. R. Laker and W. M. C. Sansen, *Design of Analog Integrated Circuits and Systems,* New York: McGraw-Hill, 1994.
4. S. J. Jou and T. L. Chen, On-chip voltage down converter for LV/LP digital, *IEEE Int. Symp. Circuits Syst.,* Hong-Kong, 1996–1999.
5. S. Kimura, Y. Imai, and Y. Miyamoto, Direct-coupled distributed baseband amplifier ICs for 40-Gb/s optical communication, *IEEE J. Solid State Circuits,* **31**: 1374–1379, 1996.
6. J. F. Gazin, *Manuel d'Applications C.I.L., Les Amplificateurs Operationnels,* 2nd ed., Arcueil, France: Thomson-CSF, Tome 1, 1974.
7. J. Millman and A. Grabel, *Microelectronics,* New York: McGraw-Hill, 1988.
8. P. R. Gray and R. G. Meyer, *Analog Integrated Circuits,* 2nd ed., New York: Wiley, 1984.
9. D. A. Johns and K. Martin, *Analog Integrated Circuit Design,* New York: Wiley, 1997.
10. Anonymous, *Low Drift Amplifiers,* National Semiconductor, Linear Brief 22, June 1973.
11. Robert J. Widlar, *Reducing DC Errors in Op-Amp,* Santa Clara, CA: National Semiconductor, Technical Paper 15, December 1980.
12. C. C. Enz and G. C. Temes, Circuit techniques for reducing the effects of op-amp imperfections: Autozeroing, double sampling, and chopper stabilisation, *Proc. IEEE* **84**: 1584–1614, 1996.
13. G. Erdi, Chopper versus bipolar op amps; an unbiased comparison, design notes n° 42 in *Application Handbook,* 1993, volume II, Milpitas, CA: Linear Technology, 1993.
14. Analog Devices, *Linear Product Data Book,* Norwood, MA, 1990.
15. Analog Devices, *Amplifier Applications Guide,* Norwood, MA, 1992.
16. D. Soderquist, The OP-07 ultra low offset voltage op amp; A bipolar op amp that challenges choppers, eliminates nulling, application note 13 in Precision Monolithics Inc. *Linear and Conversion Applications Handbook,* 1986.
17. C. Toumazou, F. J. Lidgey, and D. G. Haigh, *Analog IC Design: The Current Mode Approach,* London: Peter Peregrinus, 1990.
18. A. Fabre, O. Saaid, and H. Barthelemy, On the frequency limitations of the circuits based on 2nd generation current conveyors, *Analog Integrated Circuits Signal Process.,* **7**: 113–129, 1995.
19. A. Fabre, Gyrator implementation from commercially available transimpedance operational amplifiers, *Electron. Lett.,* **28**: 263–264, 1992.
20. A. D. Wang, The Current-feedback op amp, a high-speed building block, in *Applications Handbook,* Tucson, AZ: Burr–Brown, 1994.
21. B. Harvey, Current feedback op-amp limitations: a state of the art review, *Conf. Proc. Int. Symp. Circuits Syst.,* 1993.

ALAIN FABRE
FABRICE SEGUIN
HOUNAIDA ZOUAOUI ABOUDA
Université de Bordeaux I
HERVE BARTHELEMY
Institut Supérieur d'Electronique de la Méditerranée

DC CONVERTERS.

See HVDC POWER CONVERTERS.

DC–DC POWER CONVERTERS

Direct current–direct current (dc–dc) power converters are employed in a variety of applications, including power supplies for personal computers, office equipment, spacecraft power systems, laptop computers, and telecommunications equipment, as well as dc motor drives. The input to a dc–dc converter is an unregulated dc voltage V_g. The converter produces a regulated output voltage V, having a magnitude (and possibly polarity) that differs from V_g. For example, in a computer off-line power supply, the 120 V or 240 V alternating current (ac) utility voltage is rectified, producing a dc voltage of approximately 170 V or 340 V, respectively. A dc–dc converter then reduces the voltage to the regulated 5 V or 3.3 V required by the processor integrated circuits (ICs).

High efficiency is invariably required, since cooling of inefficient power converters is difficult and expensive. The ideal dc–dc converter exhibits 100% efficiency; in practice, efficiencies of 70% to 95% are typically obtained. This is achieved using *switched-mode,* or *chopper,* circuits whose elements dissipate negligible power. *Pulse-width modulation* (PWM) allows control and regulation of the total output voltage. This approach is also employed in applications involving alternating current, including high-efficiency dc–ac power converters (inverters and power amplifiers), ac–ac power converters, and some ac–dc power converters (low-harmonic rectifiers).

A basic dc–dc converter circuit known as the *buck converter* is illustrated in Fig. 1. A single-pole double-throw (SPDT) switch is connected to the dc input voltage V_g as shown. The switch output voltage $v_s(t)$ is equal to V_g when the switch is in position 1, and it is equal to zero when the switch is in position 2. The switch position varies periodically, such that $v_s(t)$ is a rectangular waveform having period T_s and duty

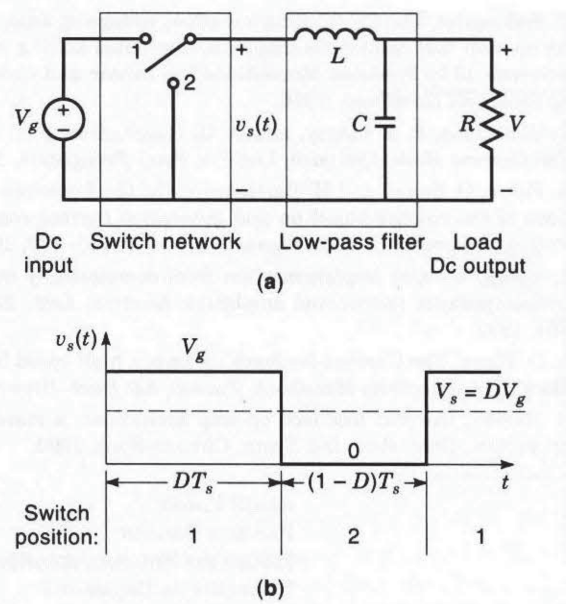

Figure 1. The buck converter consists of a switch network that reduces the dc component of voltage, along with a low-pass filter that removes the high-frequency switching harmonics: (a) schematic, (b) switch voltage waveform.

cycle D. The duty cycle is equal to the fraction of time that the switch is connected in position 1, and hence $0 \le D \le 1$. The *switching frequency* f_s is equal to $1/T_s$. In practice, the SPDT switch is realized using semiconductor devices such as diodes, power metal-oxide-semiconductor field effect transistors (MOSFETs), insulated-gate bipolar transistors (IGBTs), bipolar junction transistors (BJTs), or thyristors. Typical switching frequencies lie in the range 1 kHz to 1 MHz, depending on the speed of the semiconductor devices, the power level of the converter, and other requirements such as control loop bandwidth.

The switch network changes the dc component of the voltage. By Fourier analysis, the dc component of a waveform is given by its average value. The average value of $v_s(t)$ is given by

$$V_s = \frac{1}{T_s}\int_0^{T_s} v_s(t)\,dt = DV_g \tag{1}$$

The integral is equal to the area under the waveform, or the height V_g multiplied by the time DT_s. It can be seen that the switch network reduces the dc component of the voltage by a factor equal to the duty cycle D. Since $0 \le D \le 1$, the dc component of V_s is less than or equal to V_g.

The power dissipated by the switch network is ideally equal to zero. When the switch contacts are closed, the voltage across the contacts is equal to zero and hence the power dissipation is zero. When the switch contacts are open, there is zero current and the power dissipation is again equal to zero. Therefore, the ideal switch network is able to change the dc component of voltage without dissipation of power.

In addition to the desired dc voltage component V_s, the switch waveform $v_s(t)$ also contains undesired harmonics of the switching frequency. In most applications, these harmonics must be removed, such that the converter output voltage $v(t)$ is essentially equal to the dc component $V = V_s$. A low-

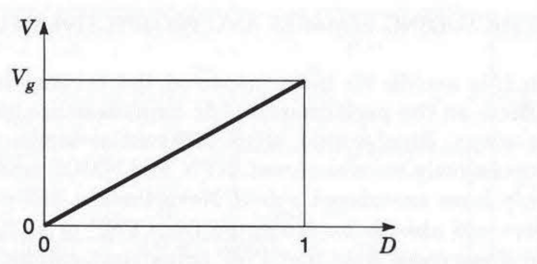

Figure 2. Buck converter dc output voltage V versus duty cycle D.

pass filter is employed for this purpose. The converter of Fig. 1 contains a single-section LC low-pass filter. The filter has corner frequency f_0 given by

$$f_0 = \frac{1}{2\pi\sqrt{LC}} \tag{2}$$

The corner frequency f_0 is chosen to be sufficiently less than the switching frequency f_s, so that the filter essentially passes only the dc component of $v_s(t)$. To the extent that the inductor and capacitor are ideal, the filter removes the switching harmonics without dissipation of power. Thus, the converter produces a dc output voltage whose magnitude is controllable via the duty cycle D, using circuit elements that (ideally) do not dissipate power.

The *conversion ratio* $M(D)$ is defined as the ratio of the dc output voltage V to the dc input voltage V_g under steady-state conditions:

$$M(D) = \frac{V}{V_g} \tag{3}$$

For the buck converter, $M(D)$ is given by

$$M(D) = D \tag{4}$$

This equation is plotted in Fig. 2. It can be seen that the dc output voltage V is controllable between 0 and V_g, by adjustment of the duty cycle D.

Figure 3 illustrates one way to realize the switch network in the buck converter, using a power MOSFET and diode. A

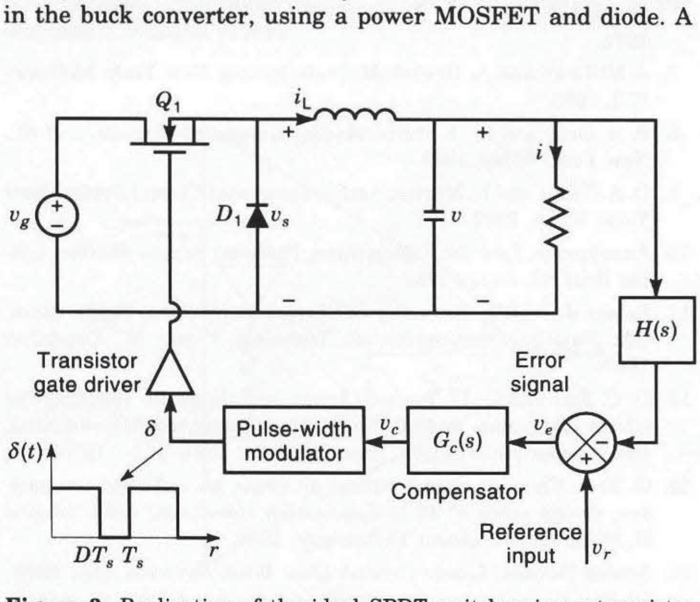

Figure 3. Realization of the ideal SPDT switch using a transistor and freewheeling diode. In addition, a feedback loop is added for regulation of the output voltage.

gate drive circuit switches the MOSFET between the conducting (on) and blocking (off) states, as commanded by a logic signal $\delta(t)$. When $\delta(t)$ is high (for $0 < t < DT_s$), MOSFET Q_1 conducts with negligible drain-to-source voltage. Hence, $v_s(t)$ is approximately equal to V_g, and the diode is reverse-biased. The positive inductor current $i_L(t)$ flows through the MOSFET. At time $t = DT_s$, $\delta(t)$ becomes low, commanding MOSFET Q_1 to turn off. The inductor current must continue to flow; hence, $i_L(t)$ forward-biases diode D_1, and $v_s(t)$ is now approximately equal to zero. Provided that the inductor current $i_L(t)$ remains positive, then diode D_1 conducts for the remainder of the switching period. Diodes that operate in this manner are called *freewheeling diodes* or "catch" diodes.

Since the converter output voltage $v(t)$ is a function of the switch duty cycle D, a control system can be constructed that varies the duty cycle to cause the output voltage to follow a given reference v_r. Figure 3 illustrates the block diagram of a simple converter feedback system. The output voltage is sensed using a voltage divider, and it is compared with an accurate dc reference voltage v_r. The resulting error signal is passed through an op-amp compensation network. The analog voltage $v_c(t)$ is next fed into a *pulse-width modulator*. The modulator produces a switched voltage waveform that controls the gate of the power MOSFET Q_1. The duty cycle D of this waveform is proportional to the control voltage $v_c(t)$. If this control system is well-designed, then the duty cycle is automatically adjusted such that the converter output voltage v follows the reference voltage v_r and is essentially independent of variations in v_g or load current.

CONVERTER CIRCUIT TOPOLOGIES

A large number of dc–dc converter circuits are known that can increase or decrease the magnitude of the dc voltage and/or invert its polarity (1–5). Figure 4 illustrates several com-

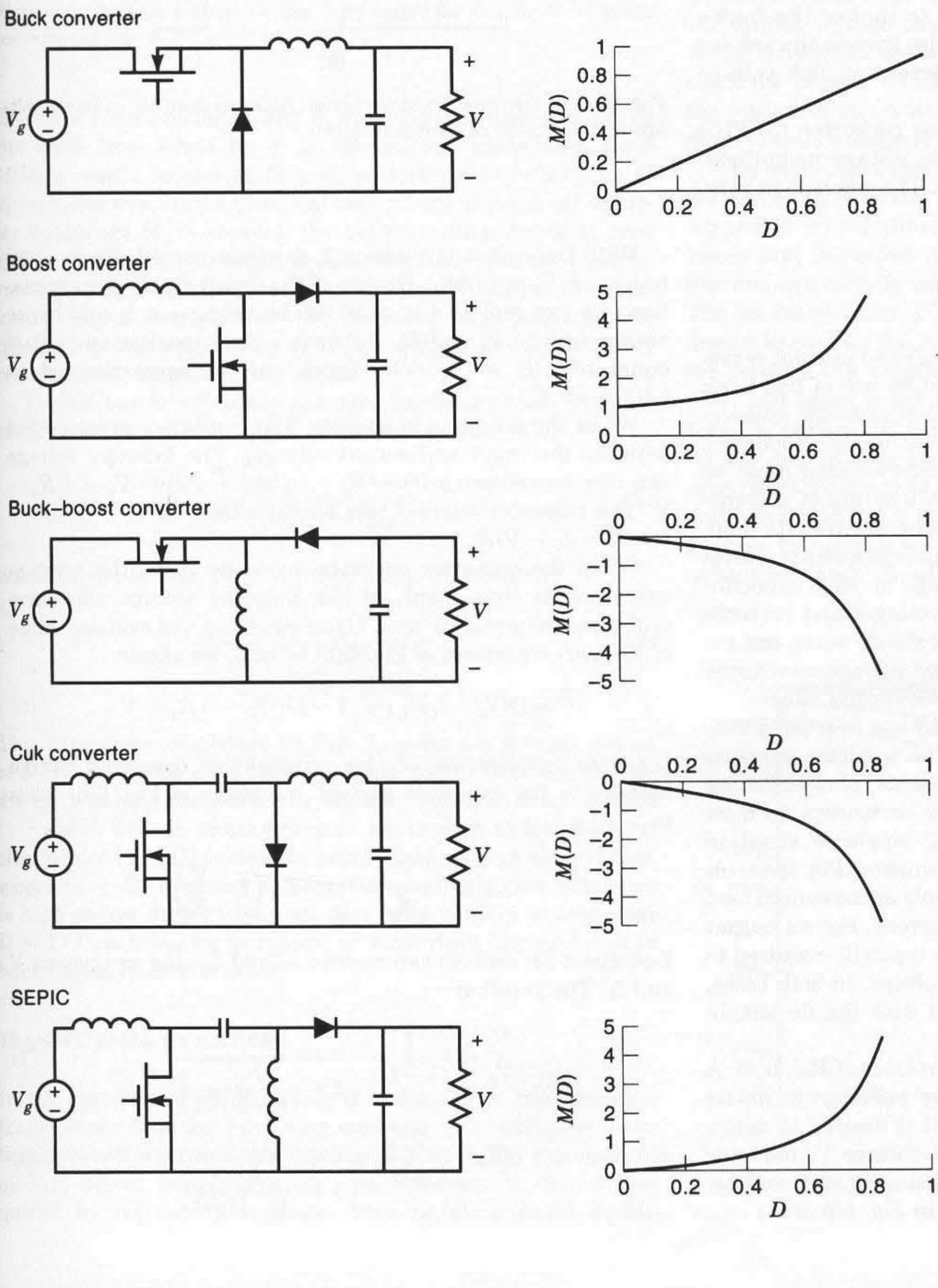

Figure 4. Several basic dc–dc converters and their dc conversion ratios $M(D) = V/V_g$.

monly used dc–dc converter circuits, along with their respective conversion ratios. In each example, the switch is realized using a power MOSFET and diode; however, other semiconductor switches such as IGBTs, BJTs, or thyristors can be substituted if desired.

The first converter is the buck converter, which reduces the dc voltage and has conversion ratio $M(D) = D$. In a similar topology known as the boost converter, the positions of the switch and inductor are interchanged. This converter produces an output voltage V that is greater in magnitude than the input voltage V_g. Its conversion ratio is $M(D) = 1/(1 - D)$.

In the buck–boost converter, the switch alternately connects the inductor across the power input and output voltages. This converter inverts the polarity of the voltage and can either increase or decrease the voltage magnitude. The conversion ratio is $M(D) = -D/(1 - D)$.

The Cuk converter contains inductors in series with the converter input and output ports. The switch network alternately connects a capacitor to the input and output inductors. The conversion ratio $M(D)$ is identical to that of the buck–boost converter. Hence, this converter also inverts the voltage polarity while either increasing or decreasing the voltage magnitude.

The single-ended primary inductance converter (SEPIC) can also either increase or decrease the voltage magnitude. However, it does not invert the polarity. The conversion ratio is $M(D) = D/(1 - D)$.

ANALYSIS OF CONVERTER WAVEFORMS

Under steady-state conditions, the voltage and current waveforms of a dc–dc converter can be found by use of two basic circuit analysis principles. The principle of *inductor volt-second balance* states that the average value, or dc component, of voltage applied across an ideal inductor winding must be zero. This principle also applies to each winding of a transformer or other multiple winding magnetic devices. Its dual, the principle of *capacitor amp-second* or *charge balance,* states that the average current that flows through an ideal capacitor must be zero. Hence, to determine the voltages and currents of dc–dc converters operating in periodic steady state, one averages the inductor current and capacitor voltage waveforms over one switching period and equates the results to zero.

The equations are greatly simplified by use of a third artifice, the *small ripple approximation.* The inductor currents and capacitor voltages contain dc components, plus *switching ripple* at the switching frequency and its harmonics. In most well-designed converters, the switching ripple is small in magnitude compared with the dc components. For inductor currents, a typical value of switching ripple at maximum load is 10% to 20% of the dc component of current. For an output capacitor voltage, the switching ripple is typically required to be much less than 1% of the dc output voltage. In both cases, the ripple magnitude is small compared with the dc component and can be ignored.

As an example, consider the boost converter of Fig. 5(a). A resistor R_L is included in series with the inductor, to model the resistance of the inductor winding. It is desired to determine simple expressions for the output voltage V, inductor current I_L, and efficiency η. Typical inductor voltage and capacitor current waveforms are sketched in Fig. 5(b).

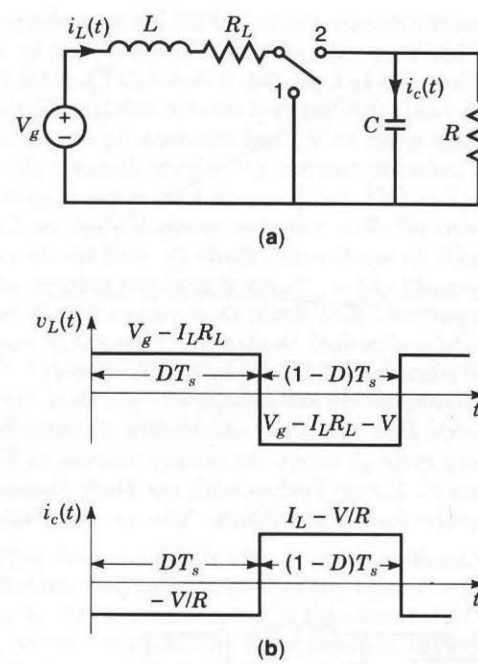

Figure 5. A nonideal boost converter: (a) schematic, (b) inductor voltage and capacitor current waveforms.

With the switch in position 1, the inductor voltage is equal to $v_L(t) = V_g - i_L(t)R_L$. By use of the small ripple approximation, we can replace $i_L(t)$ with its dc component I_L and hence obtain $v_L(t) \approx V_g - I_L R_L$. Likewise, the capacitor current is equal to $i_C(t) = -v(t)/R$, which can be approximated as $i_C(t) \approx -V/R$.

When the switch is in position 2, the inductor is connected between the input and output voltages. The inductor voltage can now be written $v_L(t) = V_g - i_L(t)R_L - v(t) \approx V_g - I_L R_L - V$. The capacitor current can be expressed as $i_C(t) = i_L(t) - v(t)/R \approx I_L - V/R$.

When the converter operates in steady state, the average value, or dc component, of the inductor voltage waveform $v_L(t)$ must be equal to zero. Upon equating the average value of the $v_L(t)$ waveform of Fig. 5(b) to zero, we obtain

$$0 = D(V_g - I_L R_L) + (1 - D)(V_g - I_L R_L - V) \tag{5}$$

Likewise, application of the principle of capacitor charge balance to the capacitor current waveform of Fig. 5(b) leads to

$$0 = D\left(-\frac{V}{R}\right) + (1 - D)\left(I - \frac{V}{R}\right) \tag{6}$$

Equations (5) and (6) can now be solved for the unknowns V and I_L. The result is

$$\frac{V}{V_g} = \frac{1}{(1-D)} \frac{1}{\left(1 + \dfrac{R_L}{(1-D)^2 R}\right)} \tag{7}$$

$$I_L = \frac{V_g}{(1-D)^2} \frac{1}{\left(1 + \dfrac{R_L}{(1-D)^2 R}\right)} \tag{8}$$

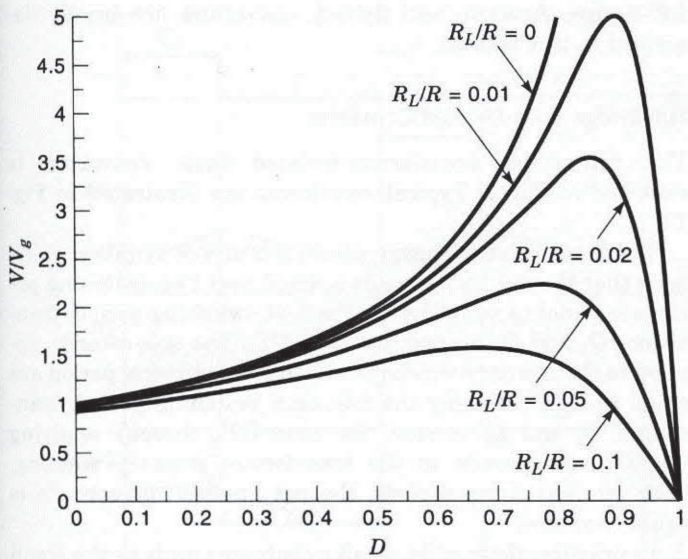

Figure 6. Output voltage versus duty cycle, for the nonideal boost converter of Fig. 5.

Equation (7) is plotted in Fig. 6, for several values of R_L/R. In the ideal case when $R_L = 0$, the voltage conversion ratio $M(D)$ is equal to one at $D = 0$, and tends to infinity as D approaches one. In the practical case where some small inductor resistance R_L is present, the output voltage tends to zero at $D = 1$. In addition, it can be seen that the inductor winding resistance R_L (and other loss elements as well) limits the maximum output voltage that the converter can produce. Obtaining a given large value of V/V_g requires that the winding resistance R_L be sufficiently small.

The converter efficiency can also be determined. For this boost converter example, the efficiency is equal to

$$\eta = \frac{P_{\text{out}}}{P_{\text{in}}} = \frac{(V^2/R)}{(V_g I_L)} \tag{9}$$

Substitution of Eqs. (7) and (8) into Eq. (9) leads to

$$\eta = \frac{1}{\left(1 + \dfrac{R_L}{(1-D)^2 R}\right)} \tag{10}$$

This expression is plotted in Fig. 7, again for several values of R_L/R. It can be seen that to obtain high efficiency, the inductor winding resistance R_L should be much smaller than $(1 - D)^2R$. This is much easier to accomplish at low-duty cycles, where $(1 - D)$ is close to unity, than at high-duty cycles, where $(1 - D)$ approaches zero. Consequently, the efficiency is high at low-duty cycles, but decreases rapidly to zero near $D = 1$. This behavior is typical of converters having boost or buck–boost characteristics.

TRANSFORMER ISOLATION

In the majority of applications, it is desired to incorporate a transformer into the switching converter, to obtain dc isolation between the converter input and output. For example, in off-line power supply applications, isolation is usually required by regulatory agencies. This isolation could be obtained by simply connecting a 50 Hz or 60 Hz transformer at the power supply ac input terminals. However, since transformer size and weight vary inversely with frequency, incorporation of the transformer into the converter can make significant improvements: The transformer then operates at the converter switching frequency of tens or hundreds of kilohertz. The size of modern ferrite power transformers is minimized at operating frequencies ranging from several hundred kilohertz to roughly 1 MHz. These high frequencies lead to dramatic reductions in transformer size.

When a large step-up or step-down conversion ratio is required, the use of a transformer can allow better converter optimization. By proper choice of the transformer turns ratio, the voltage or current stresses imposed on the transistors and diodes can be minimized, leading to improved efficiency and lower cost.

Multiple dc outputs can also be obtained in an inexpensive manner, by adding multiple secondary windings and converter secondary-side circuits. The secondary turns ratios are chosen to obtain the desired output voltages. Usually, only one output voltage can be regulated, via control of the converter duty cycle, so wider tolerances must be allowed for the auxiliary output voltages. *Cross-regulation* is a measure of the variation in an auxiliary output voltage, given that the main output voltage is regulated perfectly.

The basic operation of transformers in most power converters can be understood by replacing the transformer with the simplified model illustrated in Fig. 8. The model neglects losses and imperfect coupling between windings; such phenomena are usually considered to be converter nonidealities. The model consists of an ideal transformer plus a shunt inductor known as the magnetizing inductance L_M. This inductor models the magnetization of the physical transformer core, and hence it must obey all of the usual rules for inductors. In particular, volt-second balance must be maintained on the magnetizing inductance. Furthermore, since the voltages of all windings of the ideal transformer are proportional, volt-second balance must be maintained for each winding. Failure to achieve volt-second balance leads to transformer saturation and, usually, destruction of the converter. The

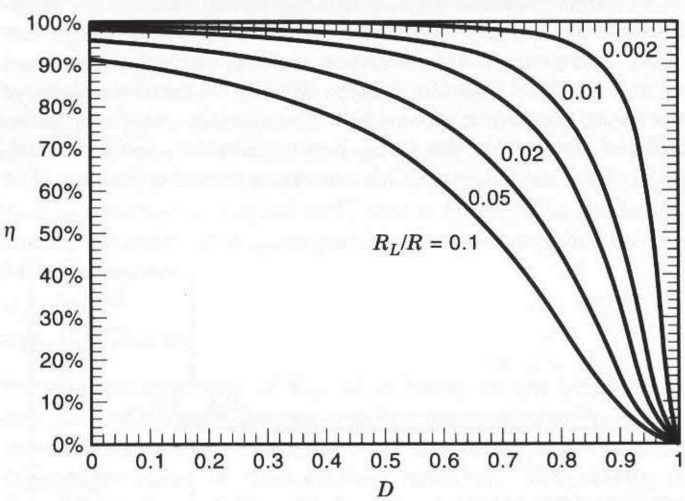

Figure 7. Efficiency versus duty cycle, for the nonideal boost converter of Fig. 5.

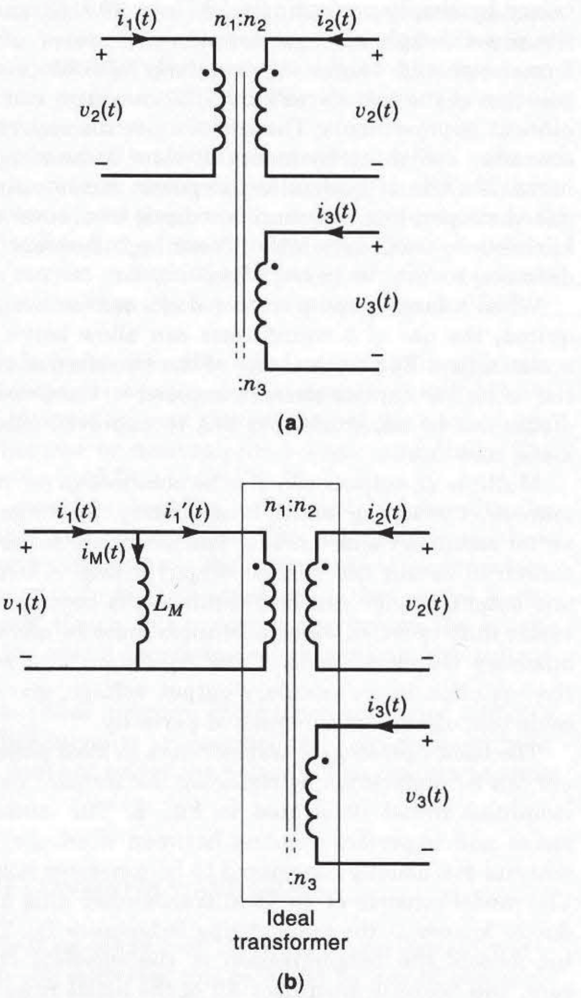

Figure 8. Modeling a physical transformer such that its basic operation within an isolated dc–dc converter can be understood: (a) transformer schematic symbol, (b) equivalent circuit model that includes magnetizing inductance L_M and an ideal transformer.

means by which transformer volt-second balance is achieved is known as the *transformer reset* mechanism.

There are several ways of incorporating transformer isolation into any dc–dc converter. The full-bridge, half-bridge, forward, and push–pull converters are commonly used isolated versions of the buck converter. Similar isolated variants of the boost converter are known. The flyback converter is an isolated version of the buck–boost converter. Isolated variants of the SEPIC and Cuk converter are also known. The full-bridge, forward, and flyback converters are briefly described in this section.

Full-Bridge Buck-Derived Converter

The full-bridge transformer-isolated buck converter is sketched in Fig. 9. Typical waveforms are illustrated in Fig. 10.

The transformer primary winding is driven symmetrically, such that the net volt-seconds applied over two switching periods is equal to zero. During the first switching period, transistors Q_1 and Q_4 conduct for time DT_s. The volt-seconds applied to the primary winding during this switching period are equal to $V_g DT_s$. During the following switching period, transistors Q_2 and Q_3 conduct for time DT_s, thereby applying $-V_g DT_s$ volt-seconds to the transformer primary winding. Over two switching periods, the net applied volt-seconds is equal to zero.

In practice, there exist small imbalances such as the small differences in the transistor forward voltage drops or transistor switching times, so that the average primary winding voltage is small but nonzero. This nonzero dc voltage can lead to transformer saturation and destruction of the converter. Transformer saturation under steady-state conditions can be avoided by placing a capacitor in series with the transformer primary. Imbalances then induce a dc voltage component across the capacitor, rather than across the transformer primary. Another solution is the use of current programmed control; the series capacitor is then omitted.

By application of the principle of volt–second balance to the output filter inductor voltage, the dc load voltage can be shown to be

$$V = nDV_g \tag{11}$$

So, as in the buck converter, the output voltage can be controlled by adjustment of the transistor duty cycle D. An additional increase or decrease of the voltage V can be obtained via the physical transformer turns ratio n.

The full-bridge configuration is typically used in switching power supplies at power levels of approximately 750 W or greater. At lower power levels, approaches such as the forward converter are preferred because of their lower parts count. The full-bridge converter requires four transistors and their associated drive circuits. The utilization of the transformer is good, leading to small transformer size. The transformer operating frequency is one-half of the transistor switching frequency.

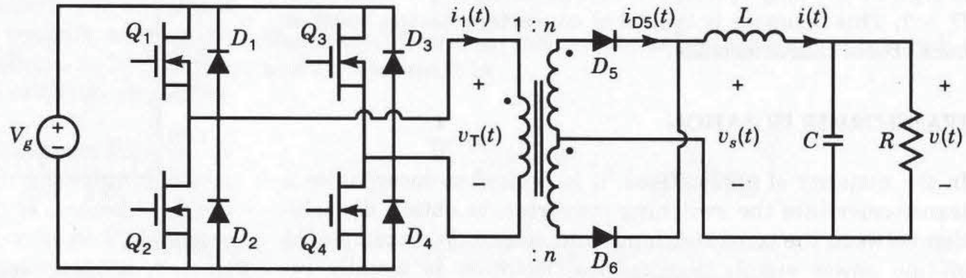

Figure 9. The full-bridge transformer-isolated buck converter.

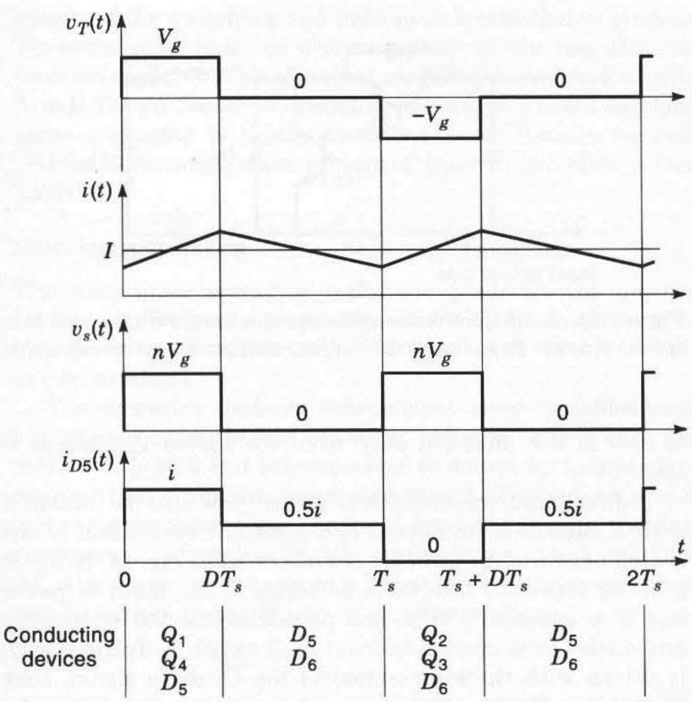

Figure 10. Waveforms of the full-bridge circuit of Fig. 9.

Forward Converter

The forward converter is illustrated in Fig. 11. This transformer-isolated converter is also based on the buck converter. It requires a single transistor, and therefore it finds application at power levels lower than those encountered in the full-bridge circuit. The maximum transistor duty cycle is limited in value; for the common choice $n_1 = n_2$, the duty cycle is limited to the range $D < 0.5$.

The transformer is reset while transistor Q_1 is in the off state. While the transistor conducts, the input voltage V_g is applied across the transformer primary winding. This causes the transformer magnetizing current to increase. When transistor Q_1 turns off, the transformer magnetizing current forward-biases diode D_1, and hence voltage $-V_g$ is applied to the second winding. This negative voltage causes the magnetizing current to decrease. When the magnetizing current reaches zero, diode D_1 turns off. Volt–second balance is maintained on the transformer windings provided that the magnetizing

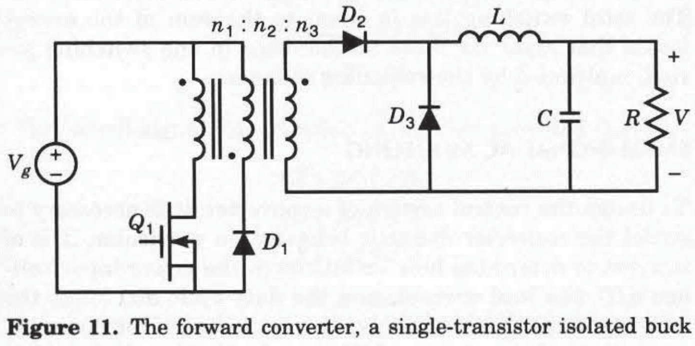

Figure 11. The forward converter, a single-transistor isolated buck converter.

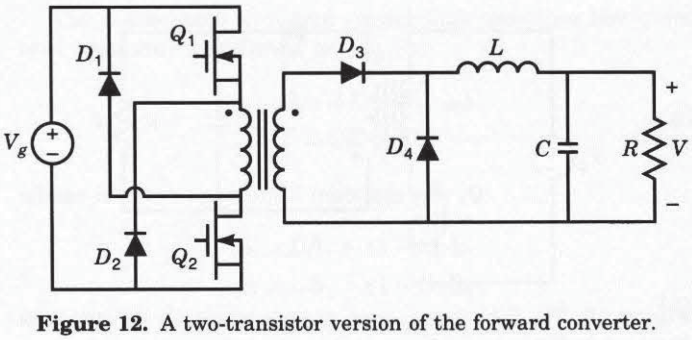

Figure 12. A two-transistor version of the forward converter.

current reaches zero before the end of the switching period. It can be shown that this occurs when

$$D \leq \frac{1}{1 + \frac{n_2}{n_1}} \tag{12}$$

For the common choice $n_2 = n_1$, this expression reduces to

$$D \leq \frac{1}{2} \tag{13}$$

Hence, the maximum duty cycle is limited. If this limit is violated, then the transistor off time is insufficient to reset the transformer. There will then be a net increase in the transformer magnetizing current over each switching period, and the transformer will eventually saturate.

The converter output voltage can be found by application of the principle of inductor volt-second balance to the output filter inductor L. The result is

$$V = \frac{n_3}{n_1} DV_g \tag{14}$$

This expression is subject to the constraint given in Eq. (12).

A two-transistor version of the forward converter is illustrated in Fig. 12. Transistors Q_1 and Q_2 are controlled by the same gate drive signal, such that they conduct simultaneously. After the transistors turn off, the transformer magnetizing current forward-biases diodes D_1 and D_2. This applies voltage $-V_g$ across the primary winding, thereby resetting the transformer. The duty cycle is again limited to $D < 0.5$. This converter has the advantage that the transistor peak blocking voltage is limited to V_g and is clamped by diodes D_1 and D_2. This circuit is quite popular in power supplies having 240 Vac inputs.

Flyback Converter

The flyback converter of Fig. 13 is based on the buck–boost converter. Although the two-winding magnetic device is represented using the same symbol as the transformer, a more descriptive name is "two-winding inductor." This device is sometimes also called a "flyback transformer." Unlike the ideal transformer, current does not flow simultaneously in

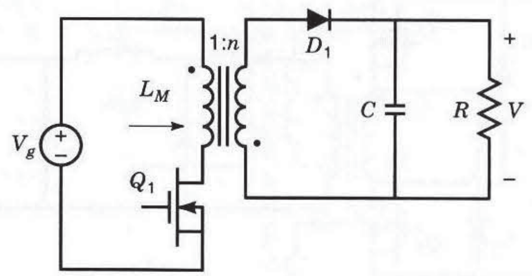

Figure 13. The flyback converter, a single-transistor isolated buck–boost converter.

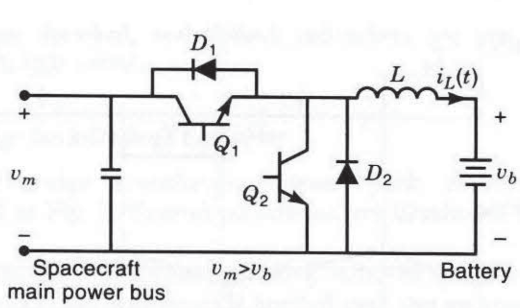

Figure 14. A buck converter with two-quadrant switches and bidirectional power flow. Spacecraft battery charger/discharger example.

both windings of the flyback transformer. Rather, the flyback transformer magnetizing inductance assumes the role of the inductor of the buck–boost converter. The magnetizing current is switched between the primary and secondary windings.

When transistor Q_1 conducts, diode D_1 is reverse-biased. The primary winding then functions as an inductor, connected to the input source V_g. Energy is stored in the magnetic field of the flyback transformer. When transistor Q_1 turns off, the current ceases to flow in the primary winding. The magnetizing current, referred to the secondary winding, now forward-biases diode D_1. Energy stored in the magnetic field of the flyback transformer is then transferred to the dc load.

Application of the principle of inductor volt-second balance to the transformer primary winding leads to the following solution for the conversion ratio of the flyback converter:

$$M(D) = \frac{V}{V_g} = n\frac{D}{(1-D)} \tag{15}$$

Thus, the conversion ratio of the flyback converter is similar to that of the buck–boost converter, but with an added factor of n.

The flyback converter has traditionally been used in the high-voltage power supplies of televisions and computer monitors. It also finds widespread application in switching power supplies at the 50 W to 100 W power range. This converter has the advantage of very low parts count. Multiple outputs can be obtained using a minimum number of added elements: Each auxiliary output requires only an additional winding, diode, and capacitor. However, in comparison with buck-derived transformer-isolated converters such as the full bridge and forward circuits, the flyback converter has the disadvantage of poor cross-regulation.

SWITCH IMPLEMENTATION

The switch network realization of Fig. 3 employs *single-quadrant* switches. Each semiconductor element is able to conduct current of only one polarity in the on state, but block voltage of one polarity in the off state. This implies that, for proper functioning of the switch network, the source voltage, load voltage, and inductor current must all be positive. Consequently, the switch network allows the instantaneous power to flow in one direction only: from the source V_g towards to load.

Bidirectional (regenerative) power flow can be obtained with a current-bidirectional *two-quadrant* realization of the switch network. An example is illustrated in Fig. 14, in which a dc–dc converter interfaces batteries to the main dc power bus of a spacecraft. The anti-parallel-connected transistors and diodes form current-bidirectional switches. Transistor Q_2 is driven with the complement of the Q_1 drive signal, such that Q_2 is off when Q_1 is on, and vice versa. To charge the battery, the inductor current $i_L(t)$ is positive and flows through transistor Q_1 and diode D_2. To discharge the battery, the current $i_L(t)$ reverses polarity and flows through transistor Q_2 and diode D_1. In both cases, the battery voltage is less than the main dc bus voltage. The magnitude and polarity of the battery current can be controlled via adjustment of the duty cycle D.

Switching loss imposes an upper limit on the switching frequencies of practical converters. During the switching transitions, the transistor voltage and current are simultaneously large. In consequence, the transistor experiences high instantaneous power loss. This can lead to significant average power loss, even though the switching transitions are short in duration. Switching loss causes the converter efficiency to decrease as the switching frequency is increased.

Several mechanisms lead to switching loss. Significant energy can be lost during the slow switching times of minority-carrier semiconductor devices such as BJTs, IGBTs, and thyristors. The diode reverse recovery process induces substantial additional energy loss in the transistor during the transistor turn-on transition. The energy stored in the semiconductor output capacitances is dissipated during the transistor turn-on transition. Energy stored in transformer leakage inductances and other stray inductances is usually dissipated by the transistor during the turn-off transition. The total switching loss is equal to the sum of the energy losses that arise via these mechanisms in one switching period, multiplied by the switching frequency.

SMALL-SIGNAL AC MODELING

To design the control system of a converter, it is necessary to model the converter dynamic behavior. In particular, it is of interest to determine how variations in the power input voltage $v_g(t)$, the load current, and the duty cycle $d(t)$ affect the output voltage. Unfortunately, understanding of converter dynamic behavior is hampered by the nonlinear time-varying nature of the switching and pulse-width modulation process. These difficulties can be overcome through the use of waveform averaging and small-signal modeling techniques (6–12). A well-known converter modeling technique known as *state-space averaging* is briefly described here. Results for several basic converters are presented later in this article (see Table 1).

State-Space Averaging

The state-space averaging technique generates the low-frequency small-signal ac equations of PWM dc–dc converters. Converter transfer functions and equivalent circuit models can be obtained.

The converter contains independent state variables such as inductor currents and capacitor voltages, which form the state vector $\boldsymbol{x}(t)$, and the converter is driven by independent sources that form the input vector $\boldsymbol{u}(t)$. The output vector $\boldsymbol{y}(t)$ contains dependent signals of interest. During the first subinterval, when the switches are in position 1 for time dT_s, the converter reduces to a linear circuit whose equations can be written in the following state-space form:

$$\begin{aligned}\frac{d\boldsymbol{x}(t)}{dt} &= \boldsymbol{A}_1\boldsymbol{x}(t) + \boldsymbol{B}_1\boldsymbol{u}(t)\\ \boldsymbol{y}(t) &= \boldsymbol{C}_1\boldsymbol{x}(t) + \boldsymbol{E}_1\boldsymbol{u}(t)\end{aligned} \tag{16}$$

The matrices $\boldsymbol{A}_1$, $\boldsymbol{B}_1$, $\boldsymbol{C}_1$, and $\boldsymbol{E}_1$ describe the network connections during the first subinterval. The duty cycle $d(t)$ may now be a time-varying quantity. During the second subinterval, the converter reduces to another linear circuit, whose state space equations are

$$\begin{aligned}\frac{d\boldsymbol{x}(t)}{dt} &= \boldsymbol{A}_2\boldsymbol{x}(t) + \boldsymbol{B}_2\boldsymbol{u}(t)\\ \boldsymbol{y}(t) &= \boldsymbol{C}_2\boldsymbol{x}(t) + \boldsymbol{E}_2\boldsymbol{u}(t)\end{aligned} \tag{17}$$

The matrices $\boldsymbol{A}_2$, $\boldsymbol{B}_2$, $\boldsymbol{C}_2$, and $\boldsymbol{E}_2$ describe the network connections during the second subinterval, of length $(1 - d)T_s$.

It is assumed that the natural frequencies of the converter network are much smaller than the switching frequency. This assumption coincides with the small ripple approximation, and it is usually satisfied in well-designed converters. It allows the high-frequency switching harmonics to be removed by an averaging process. In addition, the waveforms are linearized about a dc quiescent operating point. The converter waveforms are expressed as quiescent values plus small ac variations, as follows:

$$\begin{aligned}\boldsymbol{x}(t) &= \boldsymbol{X} + \hat{\boldsymbol{x}}(t)\\ \boldsymbol{u}(t) &= \boldsymbol{U} + \hat{\boldsymbol{u}}(t)\\ \boldsymbol{y}(t) &= \boldsymbol{Y} + \hat{\boldsymbol{y}}(t)\\ \boldsymbol{d}(t) &= \boldsymbol{D} + \hat{\boldsymbol{d}}(t)\end{aligned} \tag{18}$$

This small-signal linearization is justified provided that

$$\begin{aligned}\|\boldsymbol{X}\| &\gg \|\hat{\boldsymbol{x}}(t)\|\\ \|\boldsymbol{U}\| &\gg \|\hat{\boldsymbol{u}}(t)\|\\ \|\boldsymbol{Y}\| &\gg \|\hat{\boldsymbol{y}}(t)\|\\ D &\gg |\hat{d}(t)|\end{aligned} \tag{19}$$

where $\|\boldsymbol{x}\|$ represents the norm of vector $\boldsymbol{x}$.

The state-space averaged model that describes the quiescent converter waveforms is

$$\begin{aligned}\boldsymbol{0} &= \boldsymbol{AX} + \boldsymbol{BU}\\ \boldsymbol{Y} &= \boldsymbol{CX} + \boldsymbol{EU}\end{aligned} \tag{20}$$

where the averaged state matrices are

$$\begin{aligned}\boldsymbol{A} &= D\boldsymbol{A}_1 + (1-D)\boldsymbol{A}_2\\ \boldsymbol{B} &= D\boldsymbol{B}_1 + (1-D)\boldsymbol{B}_2\\ \boldsymbol{C} &= D\boldsymbol{C}_1 + (1-D)\boldsymbol{C}_2\\ \boldsymbol{E} &= D\boldsymbol{E}_1 + (1-D)\boldsymbol{E}_2\end{aligned} \tag{21}$$

The steady-state solution of the converter is

$$\begin{aligned}\boldsymbol{X} &= -\boldsymbol{A}^{-1}\boldsymbol{BU}\\ \boldsymbol{Y} &= (-\boldsymbol{CA}^{-1}\boldsymbol{B} + \boldsymbol{E})\boldsymbol{U}\end{aligned} \tag{22}$$

The state equations of the small-signal ac model are

$$\begin{aligned}\frac{d\boldsymbol{x}(t)}{dt} &= \boldsymbol{A}\hat{\boldsymbol{x}}(t) + \boldsymbol{B}\hat{\boldsymbol{u}}(t) + [(\boldsymbol{A}_1 - \boldsymbol{A}_2)\boldsymbol{X} + (\boldsymbol{B}_1 - \boldsymbol{B}_2)\boldsymbol{U}]\hat{d}(t)\\ \hat{\boldsymbol{y}}(t) &= \boldsymbol{C}\hat{\boldsymbol{x}}(t) + \boldsymbol{E}\hat{\boldsymbol{u}}(t) + [(\boldsymbol{C}_1 - \boldsymbol{C}_2)\boldsymbol{X} + (\boldsymbol{E}_1 - \boldsymbol{E}_2)\boldsymbol{U}]\hat{d}(t)\end{aligned} \tag{23}$$

These equations describe how small ac variations in the input vector and duty cycle excite variations in the state and output vectors.

Canonical Model

Equivalent circuit models of dc–dc converters can be constructed using the state-space averaged equations, Eqs. (20) and (23). Since all PWM dc–dc converters perform similar basic functions, one finds that the equivalent circuit models have the same form. Consequently, the *canonical circuit model* of Fig. 15 can represent the physical properties of PWM dc–dc converters.

The primary function of a dc–dc converter is the transformation of dc voltage and current levels, ideally with 100% efficiency. This function is represented in the model by an ideal *dc transformer,* denoted by a transformer symbol having a solid horizontal line. The dc transformer model has an effective turns ratio equal to the quiescent conversion ratio $M(D)$. It obeys all of the usual properties of transformers, except that it can pass dc voltages and currents. Although conventional magnetic-core transformers cannot pass dc voltages, we are nonetheless free to define an ideal dc transformer symbol;

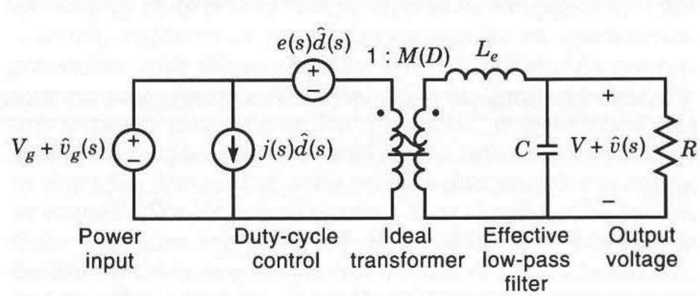

Figure 15. The canonical model: a small-signal equivalent circuit that models dc–dc converter dynamics and transfer functions.

Table 1. Canonical Model Parameters for Several Basic Converters

Converter	$M(D)$	L_e	$e(s)$	$j(s)$
Buck	D	L	$\frac{V}{D^2}$	$\frac{V}{R}$
Boost	$\frac{1}{1-D}$	$\frac{L}{(1-D)^2}$	$V\left(1-\frac{sL}{(1-D)^2R}\right)$	$\frac{V}{(1-D)^2R}$
Buck–boost	$-\frac{D}{1-D}$	$\frac{L}{(1-D)^2}$	$-\frac{V}{D^2}\left(1-\frac{sDL}{(1-D)^2R}\right)$	$-\frac{V}{(1-D)^2R}$

use of this symbol in modeling dc–dc converter properties is justified because its predictions are correct.

Small ac variations in the source voltage $v_g(t)$ are also transformed by the conversion ratio $M(D)$. Hence, a sinusoidal line is added to the dc transformer symbol, to denote that it also correctly represents how small-signal ac variations pass through the converter.

Small ac variations in the duty cycle $d(t)$ excite ac variations in the converter voltages and currents. This is modeled by the $e(s)\hat{d}$ and $j(s)\hat{d}$ generators of Fig. 15. In general, both a current source and a voltage source are required.

The converter inductors and capacitors, necessary to low-pass filter the switching harmonics, also low-pass filter ac variations. The canonical model therefore contains an effective low-pass filter. Figure 15 illustrates the two-pole low-pass filter of the buck, boost, and buck–boost converters; complex converters having additional inductors and capacitors, such as the Cuk and SEPIC, contain correspondingly complex effective low-pass filters. The element values in the effective low-pass filter do not necessarily coincide with the physical element values in the converter. In general, the element values, transfer function, and terminal impedances of the effective low-pass filter can vary with quiescent operating point.

Canonical model parameters for the ideal buck, boost, and buck–boost converters are listed in Table 1. Transformer isolated versions of the buck, boost, and buck–boost converters, such as the full-bridge, forward, and flyback converters, can also be modeled using the equivalent circuit of Fig. 15 and the parameters of Table 1; one must then correctly account for the transformer turns ratio by referring all quantities to the transformer secondary.

Small-Signal Transfer Functions of the Buck, Boost, and Buck–Boost Converters

The canonical circuit model of Fig. 15 can be solved using conventional linear circuit analysis techniques, to find quantities of interest such as the small-signal control-to-output and line-to-output transfer functions. The control-to-output transfer function $G_d(s)$ is the transfer function from $\hat{d}(s)$ to $\hat{v}(s)$, with $\hat{v}_g(s)$ set to zero. The line-to-output transfer function $G_g(s)$ is the transfer function from $\hat{v}_g(s)$ to $\hat{v}(s)$, with $\hat{d}(s)$ set to zero. For the buck, boost, and buck–boost converters, these transfer functions can be written in the following forms:

$$G_d(s) = G_{d0}\frac{\left(1-\frac{s}{\omega_z}\right)}{1+\frac{s}{Q\omega_0}+\left(\frac{s}{\omega_0}\right)^2} \tag{24}$$

$$G_g(s) = G_{g0}\frac{1}{1+\frac{s}{Q\omega_0}+\left(\frac{s}{\omega_0}\right)^2} \tag{25}$$

Expressions for the parameters of Eqs. (24) and (25) are listed in Table 2. The boost and buck–boost converters exhibit control-to-output transfer functions containing two poles and one right half-plane (nonminimum phase) zero. The buck converter $G_d(s)$ exhibits two poles but no zero. The line-to-output transfer functions of all three converters contain two poles and no zeroes.

The results of Table 2 can be applied to transformer-isolated versions of the buck, boost, and buck–boost converters, by referring all element values to the transformer secondary side. Equation (25) must also be multiplied by the transformer turns ratio.

The control systems of boost and buck–boost converters tend to be destabilized by the presence of the right-half plane (RHP) zero in the control-to-output transfer function. This occurs because during a transient the phase lag of the RHP zero causes the output to initially change in the wrong direction. When a RHP zero is present, it is difficult to obtain an adequate phase margin in conventional single-loop feedback systems having wide bandwidth. Prediction of the RHP zero, and

Table 2. Small-Signal Transfer Function Parameters for Basic dc–dc Converters

Converter	G_{g0}	G_{d0}	ω_0	Q	ω_z
Buck	D	$\frac{V}{D}$	$\frac{1}{\sqrt{LC}}$	$R\sqrt{\frac{C}{L}}$	∞
Boost	$\frac{1}{1-D}$	$\frac{V}{1-D}$	$\frac{1-D}{\sqrt{LC}}$	$(1-D)R\sqrt{\frac{C}{L}}$	$\frac{(1-D)^2R}{L}$
Buck–Boost	$-\frac{D}{1-D}$	$\frac{V}{D(1-D)}$	$\frac{(1-D)}{\sqrt{LC}}$	$(1-D)R\sqrt{\frac{C}{L}}$	$\frac{(1-D)^2R}{DL}$

the consequent explanation of why the feedback loops controlling continuous conduction mode boost and buck–boost converters tend to oscillate, was one of the early successes of averaged converter modeling and state-space averaging.

BIBLIOGRAPHY

1. R. D. Middlebrook, Power electronics: Topologies, modeling, and measurement, *Proc. IEEE Int. Symp. Circuits Syst.,* 1981, Chicago.
2. S. Cuk, Basics of switched-mode power conversion: Topologies, magnetics, and control, in *Advances in Switched-Mode Power Conversion,* R. D. Middlebrook and S. Cuk (eds.), Vol. 2, Irvine: Teslaco, 1981, pp. 279–310.
3. R. W. Erickson, *Fundamentals of Power Electronics,* New York: Chapman & Hall, 1997.
4. R. Severns and G. E. Bloom, *Modern Dc-to-Dc Switchmode Power Converter Circuits,* New York: Van Nostrand Reinhold, 1985.
5. N. Mohan, T. Undeland, and W. Robbins, *Power Electronics: Converters, Applications, and Design,* 2nd ed., New York: Wiley, 1995.
6. R. D. Middlebrook and S. Cuk, A general unified approach to modeling switching-converter power stages, *Int. J. Electron.,* **42** (6): 521–550, 1977.
7. S. Cuk, *Modeling, analysis, and design of switching converters,* Ph.D. thesis, California Institute of Technology, November 1976.
8. G. W. Wester and R. D. Middlebrook, Low frequency characterization of switched dc–dc converters, *IEEE Trans. Aerosp. Electron. Syst.,* **AES-9**: 376–385, 1973.
9. D. M. Mitchell, *Dc–Dc Switching Regulator Analysis,* New York: McGraw-Hill, 1988.
10. P. T. Krein et al., On the use of averaging for the analysis of power electronic systems, *IEEE Trans. Power Electron.,* **5** (2): 182–190, 1990.
11. A. Kislovski, R. Redl, and N. Sokal, *Dynamic Analysis of Switching-Mode DC/DC Converters,* New York: Van Nostrand Reinhold, 1994.
12. V. Vorperian, R. Tymerski, and F. C. Lee, Equivalent circuit models for resonant and PWM switches, *IEEE Trans. Power Electron.,* **4** (2): 205–214, 1989.

ROBERT W. ERICKSON
University of Colorado

DC MACHINES

Direct-current machines (dc machines) are used both as generators and motors. In the generator mode, mechanical input power at the rotating shaft is converted into electric output power at the electric terminals of the machine with an efficiency less than unity due to inevitable losses in the machine. Electrical output quantities are current and voltage. Both of them are dc values and may be used to feed electrical devices. In the motor mode, the energy flow is reversed: Electrical dc input power at the terminals is converted into mechanical output power at the rotating shaft, thus enabling the machine to drive a pump, an elevator, or a similar mechanical apparatus, again with an efficiency of less than unity.

BASIC DESCRIPTION OF DC MACHINES

These dc machines consist of a laminated iron core, fixed on a rotating shaft. An electrical armature winding is placed within slots along the circumference of the cylindrical rotor iron core near the surface; its coil ends are connected to the mechanical commutator, which consists of copper segments that are separated by electrically insulating thin mica sheets. The rotor, with its bearings mounted into bearing end shields, is rotating within the stator, which consists of several magnetic pole pairs (at least one pole pair is necessary). The stationary magnetic field of these poles in the airgap between stator and rotor induces an ac voltage (back emf) into the rotating armature winding according to Faraday's law (1,2). Carbon brushes, sliding on the commutator cylindrical surface, along with the commutator itself rectify the ac voltage, thus creating a dc voltage between two brushes of opposite electric potential. All positive brushes are connected to the positive terminal, and all negative brushes to the negative terminal likewise. If, for example, an ohmic resistor is connected to these terminals, a dc current will flow, and electric power will be dissipated as heat in the ohmic resistor. The machine is acting as a generator and needs mechanical input power to prolong the described power conversion. Inside the armature winding the current flow is—like the induced ac voltage—an ac current flow, which, along with the previously noted magnetic air-gap field, generates a constant braking torque according to Lorentz's law (1,2). Thus the mechanical input torque at the shaft, produced, for example, by a driving diesel engine, has to overcome the electromagnetic braking torque in order to generate energy flow from the diesel engine into the resistor.

By reversing the direction of power flow by reversing the direction of dc current flow outside the dc machine, one gets motor operation. For example, an external battery supply with a certain dc voltage sufficiently larger than the induced back emf to overcome the unavoidable voltage drop of internal end external electrical resistances will feed a dc current of opposite direction into the dc machine. The generated electromagnetic torque therefore also changes its direction and accelerates the rotor instead of the previously mentioned braking. Thus, the dc machine is able to drive other mechanically coupled machines such as pumps or elevators. So, both motor and generator operation are two modes of the same machine, depending on the direction of power flow.

The sliding brush–commutator mechanical contact (3) and the mechanically sensitive commutator itself put electrical and speed limitations to dc machines. Furthermore, brush wear under normal operation conditions, along with carbon dust production, requires maintenance such as changing the brushes that are too short and cleaning the machines to avoid electrical flashover within the windings due to the electrically conducting carbon dust layers. Therefore dc generators are currently replaced in many applications by ac synchronous generators with silicon rectifiers such as the electric generators in cars or rotating dc exciter units for large turbo generators in power plants (so-called "brushless" dc generators). As speed and torque of dc machines can be influenced separately by changing the applied voltage, thus changing the speed, or by changing the armature current, thus changing the torque, these machines are preferred as variable-speed drives. The control methods are simple, the produced torque is smooth, and dynamical response is very quick, as the electromagnetic time constant of the armature circuit is low. For many years these machines have been used as variable-speed drives in